UNIVERSITY OF BIRMINGHAM

University of Birmingham
Research at Birmingham

Kinetics of methyl lactate formation from the transesterification of polylactic acid catalyzed by Zn(II) complexes

Roman Ramirez, Luis; McKeown, Paul; Jones, Matthew; Wood, Joe

Document Version
Publisher's PDF, also known as Version of record

Link to publication on Research at Birmingham portal

Download date: 14. Jun. 2020

Kinetics of Methyl Lactate Formation from the Transesterification of Polylactic Acid Catalyzed by Zn(II) Complexes

Luis A. Román-Ramírez,[§] Paul McKeown,[§] Matthew D. Jones,* and Joseph Wood*

Read Online

ACCESS | Metrics & More | Article Recommendations | Supporting Information

ABSTRACT: The kinetics of the transesterification of polylactic acid (PLA) with methanol to form methyl lactate catalyzed by Zn(II) complexes was studied experimentally and numerically. The complexes, $Zn(\mathbf{1^{Et}})_2$ and $Zn(\mathbf{2^{Pr}})_2$, were synthesized from ethylenediamine and propylenediamine Schiff bases, respectively. The temperature range covered was 313.2−383.2 K. An increase in the reaction rate with the increase in temperature was observed for the $Zn(\mathbf{1^{Et}})_2$-catalyzed reaction. The temperature relationship of the rate coefficients can be explained by a linear Arrhenius dependency with constant activation energy. The kinetics of $Zn(\mathbf{2^{Pr}})_2$, on the other hand, is only explained by non-Arrhenius kinetics with convex variable activation energy, resulting in faster methyl lactate production rates at 323.2 and 343.2 K. The formation of a new catalyst species, likely through reaction with protic reagents, appears to promote the formation of intermediate complexes, resulting in the nonlinear behavior. Stirring speed induced the stability of the intermediate complexes. Contrary to $Zn(\mathbf{1^{Et}})_2$, $Zn(\mathbf{2^{Pr}})_2$ was susceptible to the presence of air/moisture in solution. The kinetic parameters were obtained by fitting the experimental data to the mass and energy balance of a consecutive second step reversible reaction taking place in a jacketed stirred batch reactor. For the case of $Zn(\mathbf{2^{Pr}})_2$, the activation energy was fitted to a four-parameter equation. The kinetic parameters presented in this work are valuable for the design of processes involving the chemical recycling of PLA into green solvents.
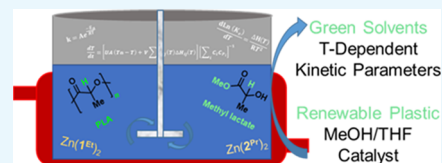
1. INTRODUCTION

Although polylactic acid (PLA) is a promising material to replace traditional synthetic polymers in packaging applications,[1] its higher cost and low natural degradation rates have limited its commercial growth.[2] Chemical recycling of PLA is an alternative to mechanical recycling and composting of postconsumer PLA, resulting in lower production costs and value-added products.[3,4] Chemical recycling methods, including pyrolysis, hydrolysis, and acid−base depolymerization, have been demonstrated in the literature;[5−12] however, these processes are characterized by high temperatures (up to 533 K). Milder operating conditions can be achieved by the catalyzed transesterification reaction of PLA to produce alkyl lactates, which are considered as green solvents because of their low toxicity and biodegradability.[13,14] Alkyl lactates are considered as substitutes to oil-derived solvents with applications in polymer manufacturing, biochemicals, pharmaceuticals, agricultural chemicals, as well as being platform chemicals, with an estimated market value of $16,800 million per annum.[13−16] For instance, propylene glycol, a monomer in the production of polyurethanes, can be obtained from the hydrogenation of methyl lactate (MeLa).[15] The potential to obtain lactide from MeLa has also been demonstrated,[17−20] opening the possibility for a circular economy.

A catalyst is normally employed to reduce the transesterification reaction temperature with a range of different examples being reported. Acid/base catalysis for the hydrolysis of PLA has been widely reported; however, this often requires harsh conditions.[21−23] Traditional acid/base catalysts have been successfully replaced by ionic liquids for PLA degradation.[24] Organocatalysts, triazabicyclodecene and 4-dimethylaminopyridine, have also been demonstrated for PLA degradation, having high activity in solution at low temperatures, as well as being able to polymerize lactide to PLA.[12,25,26] The use of commercially available complexes such as metal catalysts has been assessed at high temperatures (≥373 K).[5,27] Sobota and co-workers[5] reported a range of alkali and alkaline earth metals, such as Zn(II), Sn(II), and Al(III), for the alcoholysis of PLA. The addition of metal species allowed for degradation as low as 353 K. Liu et al.[27] have reported the use of Fe(III) chloride as a catalyst for PLA methanolysis at 403 K. Discrete metal complexes have also been applied to the alcoholysis of PLA, often in conjunction with a study into the polymerization of lactide.[28−32] Whitelaw et al.[32] have described the use of zirconium/hafnium(IV) salalen complexes for polymerization and degradation of PLA under mild conditions. Fliedel et al.[29] have reported the use of Zn(II) carbene complexes, also for polymerization and mild degradation reactions.

In a previous publication,[30] the effect of different operating parameters [PLA molecular weight (M_n), catalyst concentration, PLA particle size, stirring speed, and temperature] for the degradation of PLA into MeLa by a Zn(II) complex based on an ethylenediamine Schiff base ($Zn(1^{Et})_2$, Figure S1) was reported. Statistical analysis showed that the main variables affecting the reaction are catalyst concentration and temperature and that the reaction rate is independent of PLA M_n and stirring speed. In a recent development,[31] newly synthesized complexes based on propylenediamine Schiff base ($Zn(1^{Pr})_2$ and $Zn(2^{Pr})_2$, Figure S1) showed higher activity than $Zn(1^{Et})_2$ toward both lactide polymerization and PLA depolymerization under identical conditions, showing the potential for a faster process. In this work, temperature-dependent kinetic parameters for the depolymerization of PLA with $Zn(1^{Et})_2$ and $Zn(2^{Pr})_2$ are presented to exhibit the unexpected and unusual differences in their activity.

2. EXPERIMENTAL SECTION

2.1. Materials. *2.1.1. Small-Scale Tests.* Methanol (MeOH, HPLC grade, ≥99.9%) and tetrahydrofuran (THF) (HPLC grade, inhibitor-free, ≥99.9%) were purchased from VWR and used without further purification. Argon (≥99.998%) was purchased from BOC. PLA [VegWare Cup, M_n = 45,000 g mol^{-1} measured by gel permeation chromatography (GPC)] was cut into pieces of less than 10 mm^2.

2.1.2. Large-Scale Tests. MeOH (HPLC grade, ≥99.9%) and THF (HPLC grade, inhibitor-free, ≥99.9%) were purchased from Sigma-Aldrich and used without further purification. Nitrogen (oxygen-free, ≥99.998%) was purchased from BOC. PLA sample beads (Ingeo 2500HP and 6202D, M_n = 71,900 and 44,350 g mol^{-1}, respectively, measured by GPC) were acquired from NatureWorks and used as received unless stated otherwise. These samples covered a wide range of product applications including extrusion, thermoforming, and fibers.[33] For the experiments at 323 K and below, the beads were shredded (an RETSCH SR-300 rotor beater) to a fine form of less than 3 mm to aid dissolution.

2.2. Catalyst Synthesis and Characterization. The preparation and detailed characterization of catalysts $Zn(1^{Et})_2$, $Zn(1^{Pr})_2$, and $Zn(2^{Pr})_2$ have been reported elsewhere.[28,31] A summary of the characterization and molecular structure is provided in the Supporting Information (Figure S1 and Table S1). These catalysts were prepared under Ar/Schlenk conditions and stored under Ar in a glovebox prior to transport and use. The complexes could be prepared on a multigram scale ($Zn(1^{Et})_2$, 54 mmol scale, 72%; $Zn(1^{Pr})_2$, 21 mmol scale, 86%; and $Zn(2^{Pr})_2$, 25.5 mmol scale, 74%). Successful synthesis was confirmed by ^{1}H NMR spectroscopy for every batch prepared.

2.3. Apparatus and Procedures. *2.3.1. Small Scale.* Reactions were performed in a sealed J Young's flask under an Ar atmosphere, which had previously been dried at 393 K for at least 16 h. The reaction temperature was controlled using a silicone oil bath, and the reaction mixture was stirred by a magnetic bar.

In a typical experiment, 0.25 g of PLA was charged to a J Young's flask and taken into a glovebox. The catalyst (4 wt %, 10.4 mg) was added under the inert conditions of the glovebox and 4 mL of THF was added under a flow of Ar on a Schlenk-like condition. The flask was placed in a preheated oil bath and stirred (750 rpm) for 10 min to dissolve the polymer. The

reaction time was started when adding 1 mL of MeOH. The progress of the reaction was monitored by taking aliquots (20 μL) under an Ar flow. ^{1}H NMR analysis determined the relative molar concentrations of Internal (Int), chain-end (CE), and MeLa methine groups as detailed in ref 30 (see Figure S2 for a typical ^{1}H NMR group assignment).

Conversion of Int groups (X_{Int}), MeLa selectivity (S_{MeLa}), and MeLa yield (Y_{MeLa}) were calculated according to

$$X_{Int} = \frac{Int_0 - Int}{Int_0} \tag{1}$$

$$S_{MeLa} = \frac{MeLa}{Int_0 - Int} \tag{2}$$

$$Y_{MeLa} = S_{MeLa}X_{Int} \tag{3}$$

where Int_0 is the initial concentration of the Int groups (100%).

2.3.2. Large Scale. Reactions were performed in a 300 mL SS316 jacketed stirred batch reactor (PARR model 4566). The reaction temperature was controlled by an oil bath heating circulator (Julabo HE) connected to the jacket and a chiller (Julabo GR150) within 0.75 K. A Pt100 sensor calibrated using a three-point calibration using water as the reference fluid measured the temperature at the interior of the reactor. A control unit (PARR model 4848) monitored the stirring speed and pressure.

In a typical experiment, 12.5 g of PLA, 200 mL of THF, and 4 wt % catalyst were charged into the reactor. The reactor was sealed and the mixture was flushed with N$_2$ for 5 min at room temperature under gentle stirring. Heating was started and the stirring speed was set to 870 rpm. Once the desired operating temperature was reached and stabilized, 50 mL of MeOH was added by an HPLC pump (PerkinElmer 200) at 10 mL min^{-1}. The start of the alcohol addition marked the initial reaction time. The progress of the reaction was followed by withdrawing samples (1 mL) at different time intervals. MeLa concentration was determined by a gas chromatograph coupled with a flame-ionization detector (FID), whereas ^{1}H NMR determined the Int, CE, and MeLa groups. Reactions were carried out at 323.2, 343.2, 363.2, and 383.2 K to obtain temperature-dependent kinetic parameters.

2.3.3. Nuclear Magnetic Resonance Spectroscopy. ^{1}H NMR analysis was performed on a Bruker 400 MHz or 500 MHz spectrometer. Resonances were referenced to residual solvent signals. For the preparation of NMR samples of complexes, CDCl$_3$ was distilled and stored over molecular sieves.

2.3.4. Gas Chromatography. Quantitative analysis of the MeLa concentration was obtained by a gas chromatograph coupled with a FID (FID, Agilent Technologies, 6890N) equipped with a 30 m × 0.32 mm internal diameter and 0.25 μm film thickness capillary column (Agilent HP-5). Sample volumes (1 μL) were injected with an autosampler (Agilent Technologies, 7693A). The gas chromatography conditions were as follows: 1:100 split ratio and 423 and 523 K inlet and detector temperature, respectively. An initial oven temperature of 363 K was held for 4 min, increased to 393 K at 100 K min^{-1} and held for 1 min, and then increased to 473 K at 100 K min^{-1} and held for 2 min. Helium CP grade, purity ≥ 99.999% (BOC), was used as a carrier and makeup gas. A linear response ($R^2 > 0.998$) of the detector was obtained while measuring a multiple point external standard calibration
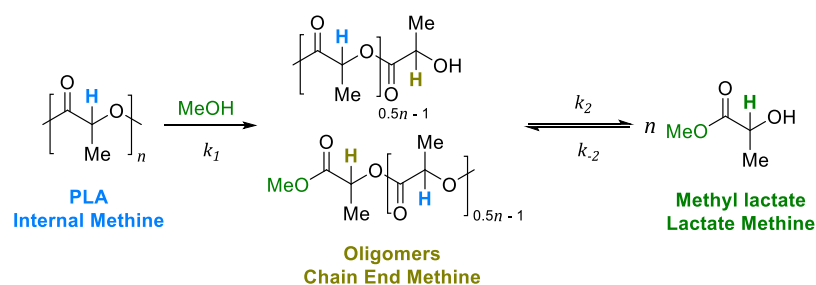
Figure 1. Methine groups determined by ^{1}H NMR for PLA (Int), Oligos (CE), and MeLa.

curve covering the 0−0.073 g mL^{-1} range. MeLa standard was purchased from Sigma-Aldrich.

3. KINETIC MODELING

3.1. Reaction Mechanism. It has been reported that the MeLa formation with $Zn(1^{Et})_2$, $Zn(Zn(1^{Pr})_2$, and $Zn(2^{Pr})_2$ catalysts follows a consecutive reaction where PLA degrades first into intermediates from which MeLa is formed through a reversible reaction.[30,31] The intermediates are believed to be composed of oligomers of relatively low molecular weight with respect to that of the original PLA, and as low as the lactate dimer. The intermediates are referred here as Oligos. The PLA, Oligos, and MeLa concentrations are represented by the concentration of Int, CE, and MeLa methine groups, respectively (Figure 1), and determined by ^{1}H NMR spectroscopy. The number of moles of PLA, Oligos, and MeLa at any given time can be calculated from the corresponding ^{1}H NMR concentrations (mol %) at that time and the initial number of moles of PLA, calculated from the initial mass of PLA and the molecular weight of the repeat unit. The concentration of MeLa calculated from ^{1}H NMR spectroscopy agreed with the gas-chromatograph-determined concentration to an average absolute error of 0.0025 g mL^{-1}. The maximum theoretical MeLa concentration for the amount of PLA used in the experiments corresponds to 0.072 g mL^{-1}. Nevertheless, because of the reversibility of the reaction, the maximum concentration observed was around 0.070 g mL^{-1}.

3.2. Mass and Energy Balance. The mass balance equations on the batch reactor are

$$\frac{dPLA}{dt} = r_{PLA} \tag{4}$$

$$\frac{dOligos}{dt} = r_{Oligos} \tag{5}$$

$$\frac{dMeLa}{dt} = r_{MeLa} \tag{6}$$

where r_i are the rate expressions for the different species given by eqs 7−9, and PLA, Oligos, and MeLa represent the molar concentrations of the respective species at any given time.

$$-r_{PLA} = k_1 PLA \tag{7}$$

$$-r_{Oligos} = r_{PLA} + r_{MeLa} \tag{8}$$

$$-r_{MeLA} = -k_2 \left(Oligos - \frac{MeLa}{K_e} \right) \tag{9}$$

In eqs 7 and 9, k_i are the rate coefficients, and the concentration equilibrium constant, $K_e = k_2/k_{-2}$, is defined with respect to MeLa. The initial conditions for the set of

ordinary differential equations (eqs 4−6) are PLA = PLA$_0$, Oligos = 0, and MeLa = 0, where PLA$_0$ is the initial molar concentration of PLA in the system.

The energy balance equation on the SS316 batch reactor is

$$\frac{dT}{dt} = \left[UA(T_a - T) + V \sum_j r_{ij}(T) \Delta H_{ij}(T) \right] \left[\sum_i C_i C_{P_i} \right]^{-1} \tag{10}$$

where $\Delta H_{ij}(T)$ is the enthalpy of reaction for the jth reaction, r_{ij} corresponds to the reaction rate expression for the ith component, and C_i and C_{P_i} are the concentration and heat capacity of the ith component, respectively.

The overall heat-transfer coefficient, U, and the heat-transfer area, A, have been estimated as 240 J s^{-1} m^{-2} K^{-1} and 0.0177 m^{-2} (see the Supporting Information). T_a is the temperature of the heat-transfer fluid whose properties are presented in Table S2. The main contributions to the heat capacity are assumed to be only those given by MeOH and THF. The average C_P was computed from a reference temperature and the current temperature, T. The C_P at any given temperature was calculated from a cubic function (eq 11) where A, B, C, and D are compound-specific coefficients (Table S3).

$$C_P = A + BT + CT^2 + DT^3 \tag{11}$$

The temperature-dependent form of K_e in eq 9 is given by the van't Hoff equation[34]

$$\frac{d \ln(K_e)}{dT} = \frac{\Delta H(T)}{RT^2} \tag{12}$$

where R is the ideal gas constant. In solving eqs 10 and 12, the change in heat capacity over the temperature range studied has been neglected (i.e., $\Delta C_P = 0$).

The temperature-dependent form of the rate coefficients was calculated using the empirical Arrhenius equation (eq 13) from which activation energies (E_a) can be readily obtained if no other thermodynamic properties are required (i.e., as is the case of the Eyring model). A in eq 13 is defined as the pre-exponential factor.

$$k = A \, e^{-E_a/RT} \tag{13}$$

Parameters ΔH_1, A, and E_a were calculated using the parameter estimation module of gPROMS ModelBuilder,[35] which uses the maximum likelihood estimation method.[35,36]

4. RESULTS AND DISCUSSION

4.1. Catalyst Stability. The stability of $Zn(1^{Et})_2$ toward moisture/oxygen in the solid state and in solution with lactide, PLA, MeOH, and MeLa has been demonstrated previously.[28,30] $Zn(1^{Et})_2$ has also been shown to remain intact

Table 1. Catalyst Activities and Reaction Rate Constants at 363.2 K[a]

catalyst	time, h	X_{Int}	S_{MeLa}	Y_{MeLa}	k_1, min^{-1}	k_2, min^{-1}	k_{-2}, min^{-1}
$Zn(1^{Et})_2$	1	66	29	19	1.9×10^{-2}	8.8×10^{-3}	4.8×10^{-3}
	5	100	62	62			
$Zn(1^{Pr})_2$	1	63	25	16	1.8×10^{-2}	7.7×10^{-3}	1.1×10^{-3}
	5	100	76	76			
$Zn(2^{Pr})_2$	1	72	29	21	2.2×10^{-2}	9.4×10^{-3}	1.5×10^{-3}
	5	100	80	80			

[a]Reaction rate constants calculated from the kinetic model presented in ref 30.

under transesterification reaction conditions.[31] Both $(Zn(1^{Pr})_2$ and $Zn(2^{Pr})_2$ were previously shown to dissociate a ligand under these conditions and form a new active species. The stability of these complexes was therefore further assessed. $Zn(1^{Pr})_2$ was found to be more air-/moisture−sensitive, showing evidence (via ^1H NMR spectroscopy) of degradation when stored in solution or in solid state. In comparison, $Zn(2^{Pr})_2$ was more stable under ambient conditions, experiencing only 2% of complex decomposition to ligand after 10 d in air (Figure S3). However, in solution (d_8-THF), more degradation is observed ($\leq$10%) even under an inert atmosphere. The formation of any other ligated zinc species was not observed under these conditions, suggesting that the formation of previously detected species is favored only under reaction conditions. These differences in stability likely resulted in the higher activities observed for $Zn(2^{Pr})_2$ in the scale-up tests, differing with the preliminary findings at the small scale.[31] Furthermore, $Zn(2^{Pr})_2$ was found to be active for the degradation of PLA in air at the small scale, achieving comparable results to that of an inert atmosphere (323 K, 1 h, X_{Int} = 100%; Y_{MeLa} = 89%). However, because of the known catalyst decomposition, further small-scale studies were performed under Ar to ensure reproducibility.

At 363.2 K, for instance, similar initial degradation rates are obtained with all catalysts, being just slightly higher for $Zn(2^{Pr})_2$, as shown in the values for the rate coefficients (Table 1). After 1 h of reaction, there are no major differences between the achieved yield with all catalysts (Table 1, Figure 2); however, as the reaction progresses, the differences become evident. After 5 h, the yield achieved by $Zn(2^{Pr})_2$ is higher than those of $Zn(1^{Pr})_2$ and $Zn(1^{Et})_2$. The formation of lactate is favored by $Zn(2^{Pr})_2$ as shown by the lower rate coefficient, k_{-2},

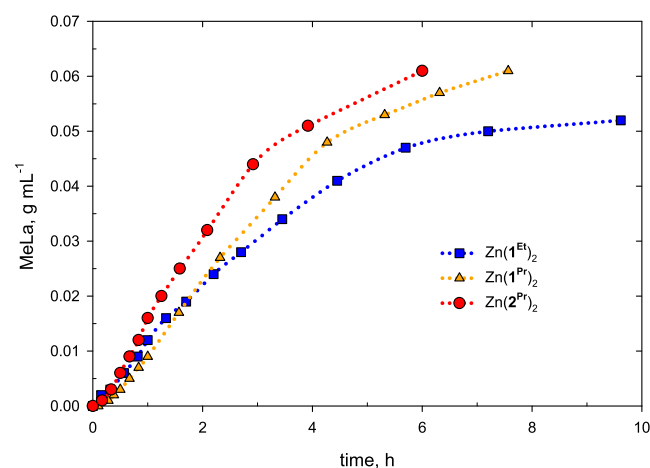for the reverse reaction. In contrast, the reformation of intermediates from the lactate is favored by $Zn(1^{Et})_2$, resulting in a lower MeLa formation rate.

Although $Zn(2^{Pr})_2$ was less susceptible to the presence of oxygen/moisture, the reaction protocol was modified to include 20 min of N_2 purging to achieve an inert atmosphere inside the reactor and to aid reproducibility of the experiments. The rest of the study was focused only on the more stable and active $Zn(2^{Pr})_2$.

4.2. Effect of Stirring Speed. Previous studies with $Zn(1^{Et})_2$ showed that this catalyst does not present mass-transfer limitations when testing two different stirring speeds (300 and 700 rpm) and two particle sizes (3 and 5 mm); although at low temperatures, the solubility of PLA in the medium has to be considered.[30] Nonetheless, two control experiments, one at 300 rpm and one at 700 rpm in air, were performed. The MeLa concentration profiles for both experiments were similar, validating the previous conclusions.

In contrast to this, testing of 700 and 870 rpm (the latter is the maximum value achieved with the current setup) on the more stable $Zn(2^{Pr})_2$ showed a direct correlation of this operating parameter with the activity of the catalyst (Figure 3). At 300 rpm, the activity of $Zn(2^{Pr})_2$ was in fact lower than that of $Zn(1^{Et})_2$, but an increase in activity was attained when increasing the stirring speed.
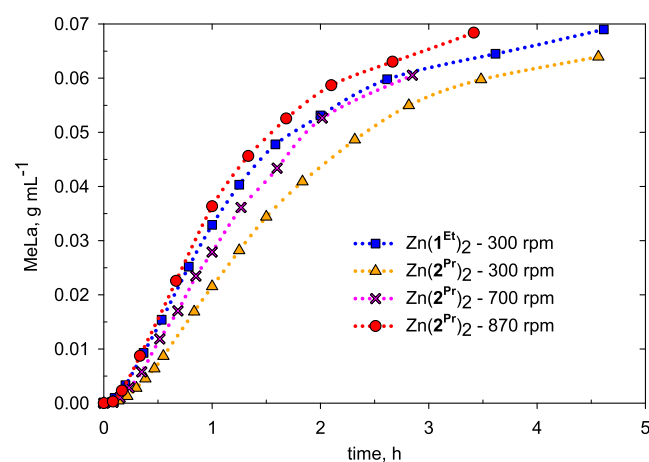
Figure 3. Effect of stirring speed on $Zn(2^{Pr})_2$ activity for the scale-up studies at 383.2 K.

4.3. Effect of Temperature and Molecular Weight. The effect of temperature on reaction rate was studied by performing experiments with the two molecular weight samples at 323.2, 343.2, 363.2, and 383.2 K (with corresponding gauge pressures of 0, 3, 130, and 330 kPa, respectively) in the 316SS batch reactor. Similar to the findings for $Zn(1^{Et})_2$,[30] the transesterification reaction catalyzed by

Figure 2. Activities of the studied catalysts at 363.2 K for the scale-up studies.

$Zn(2^{Pr})_2$ proceeded at the same rate regardless of PLA molecular weight (see for instance, Figure S4).

A clear increase in activity by the increase in temperature was observed for $Zn(1^{Et})_2$ as seen in the conversion, selectivity, and yield at 60 min (Figure 4). Conversely, higher activities were noted at lower temperatures with $Zn(2^{Pr})_2$, becoming similar to $Zn(1^{Et})_2$ at higher temperatures (Figure 4).
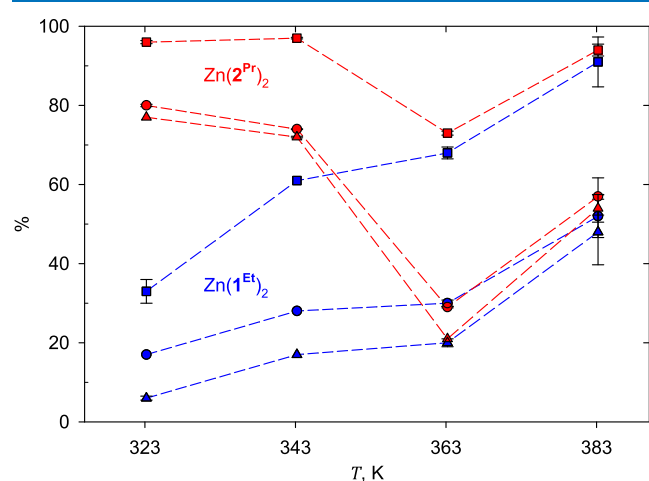

Figure 4. Conversion (■), selectivity (●), and yield (▲) at 60 min with $Zn(1^{Et})_2$ and $Zn(2^{Pr})_2$.

A plot of the reaction profiles for $Zn(2^{Pr})_2$ at the different temperatures studied provide a more insightful trend (Figure 5). The results include experiments with both PLA molecular
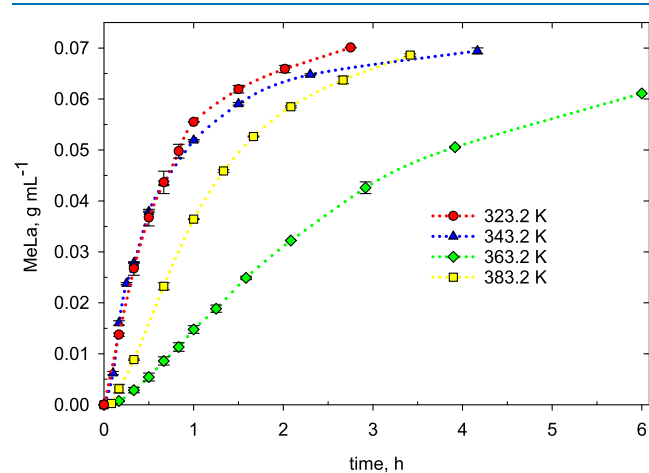

Figure 5. Effect of temperature on reaction rate with $Zn(2^{Pr})_2$. Plots include results with both PLA M_n.

weight samples. The reaction is faster at 323.2 K, with the activity decreasing with the increase of temperature, reaching a minimum around 363.2 K and then increasing again with the increase in temperature. This effect cannot be attributed to thermal catalyst decomposition in solution because the catalyst showed higher activity at 383.2 K than at 363.2 K. An additional experiment at 303.2 K showed a low initial reaction rate of 8×10^{-6} g mL^{-1} min^{-1}, which is the slowest rate observed for this reaction.

Between 313.2 and 343.2 K, the conversion, selectivity, and yield are in general in good agreement between the small and scale-up studies (Table 2). Superior activities at the small scale

Table 2. Conversion (X_{Int}), Selectivity (S_{MeLa}), and Yield (Y_{MeLa}) at the Small-Scale and Large-Scale Tests after 1 h of Reaction

T, K	J Young's flask			316SS reactor		
	X_{Int}	S_{MeLa}	Y_{MeLa}	X_{Int}	S_{MeLa}	Y_{MeLa}
313.2	95	64	61	91	36	33
323.2	100	84	84	96	80	77
333.2	100	81	81	94	56	53
343.2	100	84	84	97	74	72

can be expected because of better mixing. A constraint on the maximum attainable reaction temperature exists at the small scale because the system operates at atmospheric pressure. 343.2 K was the maximum temperature studied before witnessing boiling of the liquid mixture.

Reactions showing higher reaction rates at lower temperatures (i.e., negative E_a) are indicative of an intermediate-complex formation in a multistep reaction.[37−42] Nevertheless, the noteworthy observation in the present reaction is the curved E_a (to be detailed in Section 4.4), where starting from a relatively high temperature, the magnitude of the reaction rate coefficient decreases as temperature decreases up to a certain minimum, which then increases by decreasing the temperature further. This phenomenon has been explained to be characteristic of a system in which formation and redissociation of an initial weak complex takes place, followed by crossing of a small energy barrier to form the product.[43,44]

Based on the preliminary studies on $Zn(2^{Pr})_2$,[31] it is hypothesized that a new species is formed by the loss of one of the ligands of the catalyst through reaction with protic reagents at some temperature above 303.2 K. Once this new heteroleptic catalyst species is formed, it induces the formation of the short-lived intermediate complex at the different reaction steps. Because the PLA transesterification by $Zn(2^{Pr})_2$ involves consecutive steps with an equilibrium step, the overall reaction will be faster or slower depending on whether the temperature will promote the initial degradation step or the forward or reverse consecutive reaction.[45]

Stirring appears to induce the stabilization of the weak initial complex, therefore resulting in improved activities at higher stirring speeds; a similar effect to the pressure dependence of reaction rate due to collisional stabilization of the complex in gas-phase reactions shows negative activation energies and strongly curved Arrhenius plots.[42]

4.4. Kinetic Modeling. The enthalpy of reaction and the Arrhenius parameters for the degradation step were estimated as $\Delta H_1 = 375 \pm 69$ kJ mol^{-1}, $A_1 = 5962 \pm 7$ min^{-1}, and $E_{a_1} = 37.89 \pm 0.03$ kJ mol^{-1} (confidence intervals at 95%). The K_e at the different temperatures can be calculated from the integrated form of the van't Hoff equation, eq 12, as follows

$$\ln(K_e) = 2.3942 - \frac{288.53}{T} \qquad (14)$$

Equation 14 contains the value of enthalpy of reaction ($\Delta H_2 = 2.40 \pm 0.3$ kJ mol^{-1} with respect to MeLa), computed from the slope of $\ln(K_e)$ versus $1/T$ (Figure S5) from the fitted parameters for k_2 and k_{-2} (Table S4). The reaction rate coefficients for $Zn(1^{Et})_2$ show a linear dependency with temperature (Figure S6), with constant positive activation energy ($E_{a_2} = 39.6$ kJ mol^{-1} and $E_{a_{-2}} = 37.2$ kJ mol^{-1}).

In contrast to $Zn(1^{Et})_2$, the system with $Zn(2^{Pr})_2$ depicted a nonlinear relationship when plotting $\ln(k)$ versus $(1/T)$ (Figures 6 and S7); therefore, it is classified as exhibiting a
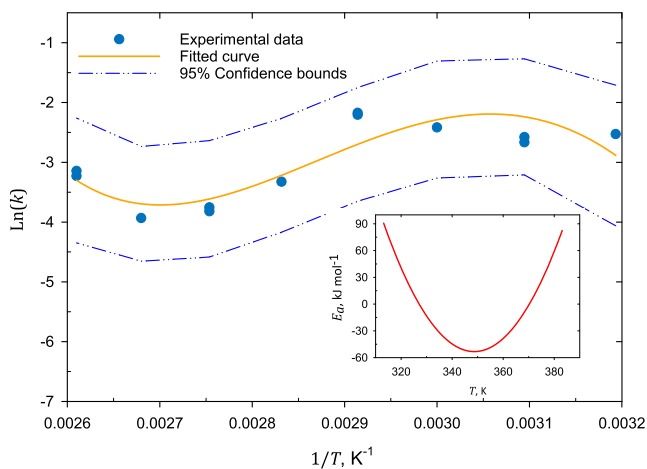

Figure 6. Curved Arrhenius plot for the rate coefficient of the degradation step and corresponding variable activation energy (inset) given by eq 16.

curved Arrhenius plot with variable (temperature-dependent) E_a.[39,42,45−48] In Figures 6 and S7, additional experiments at 313.2, 333.2, 353.2, and 373.2 K are included.

Variable E_a was recognized in the 1900s[45,47,49] and was widely studied by Perlmutter-Hayman[48] who presented a comprehensive analysis of the phenomenon and the inherent thermodynamic processes. Several examples can be found in the literature displaying curved Arrhenius plots.[43,45−57] The reaction media plays an important part on the non-Arrhenius behavior; therefore, it is more commonly observed in complex liquid-phase reactions, particularly those involving solvolysis reactions.[48,58] A few unimolecular gas-phase reactions, however, have been shown to follow non-Arrhenius kinetics.[39,45]

The variation of the rate coefficients with temperature was adjusted to a four-parameter equation (eq 15) of the type proposed by Hyne and Robertson.[59] The consequent E_a (Figure 6) is then given by eq 16. The relationship of the parameters in eq 15 with thermodynamic properties of activation (standard entropies, enthalpies, and heat capacities) has been detailed by Perlmutter-Hayman.[48] The estimated values (Table 3) are only valid on the temperature range studied,[58] that is, 313.2−383.2 K.

$$\ln(k) = \alpha T + \beta \ln T - \frac{\gamma}{T} + \delta \tag{15}$$

$$E_{a_1} = 114.141T^2 - 79,594.33T + 13,822,672 \tag{16}$$

Table 3. Parameters in Eq 15 for the Rate Coefficients with $Zn(2^{Pr})_2$[a]

	α	$\beta \times 10^{-3}$	$\gamma \times 10^{-6}$	$\delta \times 10^{-4}$
$\ln(k_1)$	13.7281	−9.5730	1.6625	5.6020
$\ln(k_2)$	23.9606	−16.7225	2.9090	9.7880
$\ln(k_{-2})$	11.3484	−8.1275	1.4473	4.7768

[a]Values estimated using the parameter estimation module of MATLAB.[60]

Contrary to what would be expected, the PLA degradation step was favored at low temperatures (below 343.2 K); in fact, the model reveals a minimum $E_{a_1} = -53$ kJ mol^{-1} at 348.6 K (Figure 6). Equation 15 implies a linear relationship of the heat capacity of activation $(\Delta C_P^{\ddagger})$, defined as the standard heat capacity change associated with the activation process, with temperature according to[58]

$$\Delta C_P^{\ddagger} \,(\text{kJ mol}^{-1}\,\text{K}^{-1}) = -79.602T - 0.228 \tag{17}$$

It is worth mentioning that $\Delta C_P^{\ddagger}$ is neglected in the Arrhenius equation model,[45,61] which is the case for $Zn(1^{Et})_2$.

The MeLa formation from the intermediates was faster at 323.2 K. The data show a decrease in the rate coefficient with an increase in temperature. The model indicates an inflection point of 347.9 K and a minimum at 368.0 K, from which the reaction rate then increases with the increase in temperature. The reverse reaction is also favored at low temperatures, and the rate coefficients are 1 order of magnitude smaller at 383.2 K compared with 323.2 K, with E_{a_2} shifting from positive to negative at 358.1 K. The average activation energies for the temperature range studied are $E_{a_1} = -5.7$ kJ mol^{-1}, $E_{a_2} = 10.5$ kJ mol^{-1}, and $E_{a_3} = -17.1$ kJ mol^{-1}, noticeably lower than the values for $Zn(1^{Et})_2$.

The higher activity of $Zn(2^{Pr})_2$ over $Zn(1^{Et})_2$ at the low temperatures can be appreciated in the magnitudes of the rate coefficients. For instance, at 343.2 K, the rate coefficients for $Zn(2^{Pr})_2$ are 1 order of magnitude higher than those of $Zn(1^{Et})_2$ ($k_1 = 0.112$ min^{-1}, $k_2 = 0.0439$ min^{-1}, $k_{-2} = 0.00584$ min^{-1} vs $k_1 = 0.0102$ min^{-1}, $k_2 = 0.0044$ min^{-1}, and $k_{-2} = 0.00093$ min^{-1}). Figure 7 displays the reaction profiles at this condition with both catalysts.

An interesting observation during the experimental studies with $Zn(2^{Pr})_2$ was that the aliquots for the experiments at 343.2 K and below continued reacting even when stored at 253.2 K, in air, without stirring. The concentration of MeLa for the initial samples almost doubled in around 72 h.

To confirm these observations, a small-scale experiment was performed for both $Zn(2^{Pr})_2$ and $Zn(1^{Et})_2$. To reach a similar starting concentration of products, transesterification was performed at 323.2 K for 15 min and 4.5 h, respectively, and this was confirmed by ^{1}H NMR analysis. The aliquots were then kept at 253.2 K, in air, and their concentrations were measured after 60 min and 72 h. The concentration of MeLa for the $Zn(2^{Pr})_2$ sample increased by 67% in 72 h, compared to only 7% for the $Zn(1^{Et})_2$ case (Figures 8 and S8). Remarkably, the main factor contributing to the increase in alkyl lactate concentration for the $Zn(2^{Pr})_2$ case is the significant degradation of PLA to intermediates. For $Zn(1^{Et})_2$, there were no further signs of polymer degradation and the only contribution to the increase in lactate concentration was due to the existing amount of intermediates. An additional local maxima of the degradation rate coefficient may exist below 313 K, but the new active catalytic species has to be created first at some temperature above 303 K.

Reaction media conditions, including solvent type and temperature range, are important parameters in the observation of variable E_a.[39] Given that the only difference between the reactions catalyzed by $Zn(1^{Et})_2$ and $Zn(2^{Pr})_2$ was the catalyst itself, the observation of variable E_a can be attributed to a lowering of the activation energy threshold by different
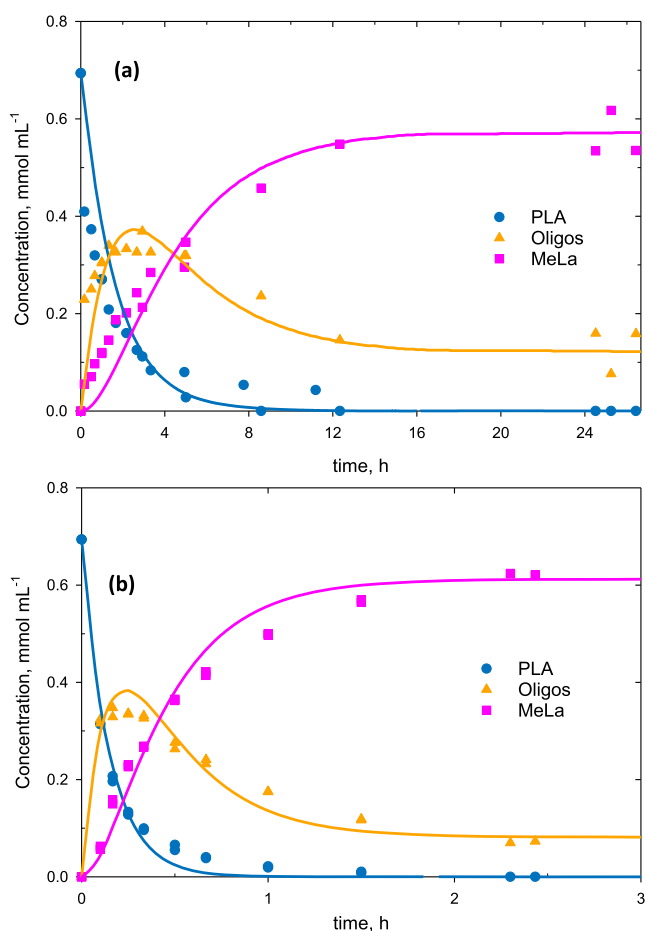
Figure 7. Reaction profiles at 343.2 K, catalyzed by (a) $Zn(1^{Et})_2$ and (b) $Zn(2^{Pr})_2$.

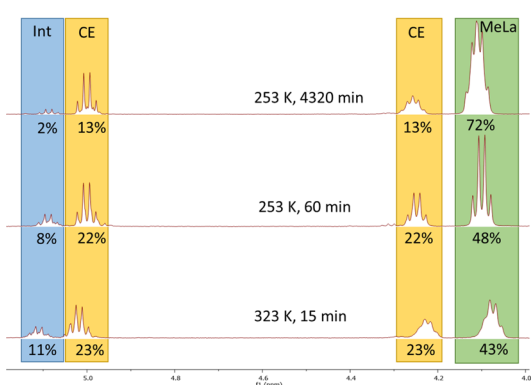**Figure 8.** ^1H NMR (C_6D_6, 400 MHz) stacked spectra and corresponding concentrations from the $Zn(2^{Pr})_2$ degradation tests at 253.2 K.

complex mechanisms, including alternative reaction paths, consecutive steps, pre-equilibria, and tunneling.[45,48,58,62]

5. CONCLUSIONS

The kinetics of the chemical degradation of PLA to form MeLa by two Zn(II) complexes were studied experimentally and numerically. The reaction mechanism with both catalysts can be explained by a consecutive reaction with the reversible second step. Similarly, the reaction rate for both catalysts was found to be independent of polymer molecular weight, an

important aspect for the industrial application of the chemical recycling of PLA of varying molecular weight.

The Zn complex from the ethylenediamine Schiff base did not show mass-transfer limitations and is not susceptible to the presence of oxygen and or moisture either in the solid state or in solution. The rate coefficients for the catalyzed reaction follow the linear temperature-dependent model given by the Arrhenius equation with constant positive activation energy.

The propylenediamine Schiff base Zn complex on the other hand is more susceptible to the presence of oxygen and or moisture when in solution but not in the solid state. The catalyzed reaction exhibits non-Arrhenius behavior with variable activation energy, resulting in faster MeLa production rates at low temperatures. While PLA starts degrading at some temperature above 303.2 K, the optimum temperature is found to be 348.6 K. Once the oligomers are formed, the reaction proceeds faster at lower temperatures. MeLa formation was observed even at subzero temperatures mainly driven by the ongoing PLA degradation.

The variable activation energy of the reaction catalyzed by $Zn(2^{Pr})_2$ is attributed to the formation of a new species by the dissociation of one ligand through reaction with protic reagents above 303.2 K, which induces the formation of an intermediate catalyst complex and to the reaction mechanism involving a consecutive reaction as well as reaction media. The system also shows collision stability as determined by the effect of stirring speed on reaction rate. Nevertheless, the activities of both catalysts tend to become similar at high temperatures.

The temperature-dependent kinetic parameters presented in this work are valuable for engineering design of processes for the degradation of PLA by Zn(II) complexes. An optimum design for the formation of MeLa from the degradation of PLA could involve the use of $Zn(2^{Pr})_2$ where the polymer is initially degraded at around 348 K then followed by a reaction at lower temperature (possibly room temperature) where MeLa is rapidly formed.

■ ASSOCIATED CONTENT

Ⓢ Supporting Information

The Supporting Information is available free of charge at https://pubs.acs.org/doi/10.1021/acsomega.0c00291.

Catalyst structure, ^1H NMR assignments, heat-transfer coefficient and heat capacity data, catalyst stability results, Arrhenius parameters and enthalpy of reaction, effect of PLA M_n, reaction rate coefficients, and ^1H NMR spectra of the degradation tests (PDF)

■ AUTHOR INFORMATION

Corresponding Authors

Matthew D. Jones − *Department of Chemistry, University of Bath, Bath BA2 7AY, U.K.;* ⓘ orcid.org/0000-0001-5991-5617; Phone: +44 (0)1225 384908; Email: mj205@bath.ac.uk; Fax: +44 (0)1225 386231

Joseph Wood − *School of Chemical Engineering, University of Birmingham, Birmingham B15 2TT, U.K.;* ⓘ orcid.org/0000-0003-2040-5497; Phone: +44 (0) 121 414 5295; Email: j.wood@bham.ac.uk; Fax: +44 (0) 121 414 5324

Authors

Luis A. Román-Ramírez − *School of Chemical Engineering, University of Birmingham, Birmingham B15 2TT, U.K.*

Paul McKeown − *Department of Chemistry, University of Bath, Bath BA2 7AY, U.K.*

Complete contact information is available at:
https://pubs.acs.org/10.1021/acsomega.0c00291

■ REFERENCES

(1) Rabnawaz, M.; Wyman, I.; Auras, R.; Cheng, S. A roadmap towards green packaging: The current status and future outlook for polyesters in the packaging industry. *Green Chem.* **2017**, *19*, 4737−4753.

(2) Haider, T. P.; Völker, C.; Kramm, J.; Landfester, K.; Wurm, F. R. Plastics of the future? The impact of biodegradable polymers on the environment and on society. *Angew. Chem., Int. Ed.* **2019**, *58*, 50−62.

(3) Hong, M.; Chen, E. Y.-X. Chemically recyclable polymers: A circular economy approach to sustainability. *Green Chem.* **2017**, *19*, 3692−3706.

(4) Payne, J.; McKeown, P.; Jones, M. D. A circular economy approach to plastic waste. *Polym. Degrad. Stab.* **2019**, *165*, 170−181.

(5) Petrus, R.; Bykowski, D.; Sobota, P. Solvothermal alcoholysis routes for recycling polylactide waste as lactic acid esters. *ACS Catal.* **2016**, *6*, 5222−5235.

(6) Piemonte, V.; Gironi, F. Kinetics of hydrolytic degradation of PLA. *J. Polym. Environ.* **2013**, *21*, 313−318.

(7) Zou, H.; Yi, C.; Wang, L.; Liu, H.; Xu, W. Thermal degradation of poly(lactic acid) measured by thermogravimetry coupled to fourier transform infrared spectroscopy. *J. Therm. Anal. Calorim.* **2009**, *97*, 929.

(8) Jehanno, C.; Pérez-Madrigal, M. M.; Demarteau, J.; Sardon, H.; Dove, A. P. Organocatalysis for depolymerisation. *Polym. Chem.* **2019**, *10*, 172−186.

(9) Herrera-Kao, W. A.; Loría-Bastarrachea, M. I.; Pérez-Padilla, Y.; Cauich-Rodríguez, J. V.; Vázquez-Torres, H.; Cervantes-Uc, J. M. Thermal degradation of poly(caprolactone), poly(lactic acid), and poly(hydroxybutyrate) studied by TGA/FTIR and other analytical techniques. *Polym. Bull.* **2018**, *75*, 4191−4205.

(10) Lv, S.; Zhang, Y.; Tan, H. Thermal and thermo-oxidative degradation kinetics and characteristics of poly (lactic acid) and its composites. *Waste Manage.* **2019**, *87*, 335−344.

(11) Cristina, A. M.; Sara, F.; Fausto, G.; Vincenzo, P.; Rocchina, S.; Claudio, V. Degradation of post-consumer PLA: Hydrolysis of polymeric matrix and oligomers stabilization in aqueous phase. *J. Polym. Environ.* **2018**, *26*, 4396−4404.

(12) Leibfarth, F. A.; Moreno, N.; Hawker, A. P.; Shand, J. D. Transforming polylactide into value-added materials. *J. Polym. Sci., Part A: Polym. Chem.* **2012**, *50*, 4814−4822.

(13) Calvo-Flores, F. G.; Monteagudo-Arrebola, M. J.; Dobado, J. A.; Isac-Garcia, J. Green and bio-based solvents. *Top. Curr. Chem.* **2018**, *376*, 18.

(14) Planer, S.; Jana, A.; Grela, K. Ethyl lactate: A green solvent for olefin metathesis. *ChemSusChem* **2019**, *12*, 4655−4661.

(15) Stadler, B. M.; Wulf, C.; Werner, T.; Tin, S.; de Vries, J. G. Catalytic approaches to monomers for polymers based on renewables. *ACS Catal.* **2019**, *9*, 8012−8067.

(16) NREL. *Chemicals from Biomass: A Market Assessment of Bioproducts with Near-Term Potential*; National Renewable Energy Laboratory, March, 2016.

(17) De Clercq, R.; Dusselier, M.; Poleunis, C.; Debecker, D. P.; Giebeler, L.; Oswald, S.; Makshina, E.; Sels, B. F. Titania-Silica Catalysts for Lactide Production from Renewable Alkyl Lactates: Structure-Activity Relations. *ACS Catal.* **2018**, *8*, 8130−8139.

(18) De Clercq, R.; Dusselier, M.; Makshina, E.; Sels, B. F. Catalytic gas-phase production of lactide from renewable alkyl lactates. *Angew. Chem., Int. Ed.* **2018**, *57*, 3074−3078.

(19) Brei, V.; Varvarin, A.; Svetlana, L.; Ya, G. Vapor-phase synthesis of lactide from ethyl lactate over TiO_2/SiO_2 catalyst. *Ukr. Biochem. J.* **2019**, *85*, 31−37.

(20) Upare, P. P.; Hwang, Y. K.; Chang, J.-S.; Hwang, D. W. Synthesis of lactide from alkyl lactate via a prepolymer route. *Ind. Eng. Chem. Res.* **2012**, *51*, 4837−4842.

(21) Brake, L. D. Preparation of alkyl esters by depolymerization. U.S. Patent 5264617 A, 1993.

(22) Coszach, P.; Bogaert, J.-C.; Willocq, J. Chemical recycling of PLA by hydrolysis. U.S. Patent 20120142958 A1, 2012.

(23) Codari, F.; Lazzari, S.; Soos, M.; Storti, G.; Morbidelli, M.; Moscatelli, D. Kinetics of the hydrolytic degradation of poly(lactic acid). *Polym. Degrad. Stab.* **2012**, *97*, 2460−2466.

(24) Song, X.; Bian, Z.; Hui, Y.; Wang, H.; Liu, F.; Yu, S. Zn-acetate-containing ionic liquid as highly active catalyst for fast and mild methanolysis of poly(lactic acid). *Polym. Degrad. Stab.* **2019**, *168*, 108937.

(25) Alberti, C.; Damps, N.; Meißner, R. R. R.; Enthaler, S. Depolymerization of end-of-life poly(lactide) via 4-dimethylamino-pyridine-catalyzed methanolysis. *ChemistrySelect* **2019**, *4*, 6845−6848.

(26) Liu, F.; Guo, J.; Zhao, P.; Gu, Y.; Gao, J.; Liu, M. Facile synthesis of DBU-based protic ionic liquid for efficient alcoholysis of waste poly(lactic acid) to lactate esters. *Polym. Degrad. Stab.* **2019**, *167*, 124−129.

(27) Liu, H.; Song, X.; Liu, F.; Liu, S.; Yu, S. Ferric chloride as an efficient and reusable catalyst for methanolysis of poly(lactic acid) waste. *J. Polym. Res.* **2015**, *22*, 135.

(28) McKeown, P.; McCormick, S. N.; Mahon, M. F.; Jones, M. D. Highly active Mg(II) and Zn(II) complexes for the ring opening polymerisation of lactide. *Polym. Chem.* **2018**, *9*, 5339−5347.

(29) Fliedel, C.; Vila-Viçosa, D.; Calhorda, M. J.; Dagorne, S.; Avilés, T. Dinuclear zinc-N-heterocyclic carbene complexes for either the controlled ring-opening polymerization of lactide or the controlled degradation of polylactide under mild conditions. *ChemCatChem* **2014**, *6*, 1357−1367.

(30) Román-Ramírez, L. A.; McKeown, P.; Jones, M. D.; Wood, J. Poly(lactic acid) degradation into methyl lactate catalyzed by a well-defined Zn(II) complex. *ACS Catal.* **2019**, *9*, 409−416.

(31) McKeown, P.; Román-Ramírez, L. A.; Bates, S.; Wood, J.; Jones, M. D. Zinc complexes for PLA formation and chemical recycling: Towards a circular economy. *ChemSusChem* **2019**, *12*, 5233−5238.

(32) Whitelaw, E. L.; Davidson, M. G.; Jones, M. D. Group 4 salalen complexes for the production and degradation of polylactide. *Chem. Commun.* **2011**, *47*, 10004−10006.

(33) NatureWorks, https://www.natureworksllc.com (October 9, 2019).

(34) Fogler, H. S. *Elements of Chemical Reaction Engineering*, 5th ed.; Pearson Prentice Hall: Boston, USA, 2016.

(35) Process Systems Enterprise Ltd.. gPROMS ModelBuilder, 5.1.1, 2019, https://www.psenterprise.com/products/gproms/modelbuilder.

(36) Aldrich, J. R.A. Fisher and the making of maximum likelihood 1912-1922. *Stat. Sci.* **1997**, *12*, 162−176.

(37) Atkins, P.; de Paula, J. *Elements of Physical Chemistry*, 5th ed.; W. H. Freeman and Company: Great Britain, 2009.

(38) Carvalho-Silva, V. H.; Coutinho, N. D.; Aquilanti, V. Temperature dependence of rate processes beyond Arrhenius and Eyring: Activation and transitivity. *Front. Chem.* **2019**, *7*, 380.

(39) Vyazovkin, S. A time to search: Finding the meaning of variable activation energy. *Phys. Chem. Chem. Phys.* **2016**, *18*, 18643−18656.

(40) Vyazovkin, S. *Isoconversional Kinetics of Thermally Stimulated Processes* [online]; Springer: Cham, Switzerland, 2015.

(41) Revell, L. E.; Williamson, B. E. Why are some reactions slower at higher temperatures? *J. Chem. Educ.* **2013**, *90*, 1024−1027.

(42) Mozurkewich, M.; Benson, S. W. Negative activation energies and curved Arrhenius plots. 1. Theory of reactions over potential wells. *J. Phys. Chem.* **1984**, *88*, 6429−6435.

(43) Sims, I. R.; Smith, I. W. M. Gas-phase reactions and energy transfer at very low temperatures. *Annu. Rev. Phys. Chem.* **1995**, *46*, 109−138.

(44) Sims, I. R. Tunnelling in space. *Nat. Chem.* **2013**, *5*, 734−736.

(45) Hulett, J. R. Deviations from the Arrhenius equation. *Q. Rev., Chem. Soc.* **1964**, *18*, 227−242.

(46) Vyazovkin, S. On the phenomenon of variable activation energy for condensed phase reactions. *New J. Chem.* **2000**, *24*, 913−917.

(47) Logan, S. R. The origin and status of the Arrhenius equation. *J. Chem. Educ.* **1982**, *59*, 279.

(48) Perlmutter-Hayman, B. The temperature-dependence of E_a. In *Progress in Inorganic Chemistry*; Lippard, S. J., Ed.; John Wiley and Sons, Inc.: USA, 1976; Vol. 20, pp 229−297.

(49) Moelwyn-Hughes, E. A. *The Chemical Statics and Kinetics of Solutions*; Academic Press Inc.: London, 1971; p 530.

(50) Aquilanti, V.; Coutinho, N. D.; Carvalho-Silva, V. H. Kinetics of low-temperature transitions and a reaction rate theory from non-equilibrium distributions. *Philos. Trans. R. Soc., A* **2017**, *375*, 20160201.

(51) Rueda-Ordóñez, Y. J.; Tannous, K. Isoconversional kinetic study of the thermal decomposition of sugarcane straw for thermal conversion processes. *Bioresour. Technol.* **2015**, *196*, 136−144.

(52) Silva, V. H. C.; Aquilanti, V.; de Oliveira, H. C. B.; Mundim, K. C. Uniform description of non-Arrhenius temperature dependence of reaction rates, and a heuristic criterion for quantum tunneling vs classical non-extensive distribution. *Chem. Phys. Lett.* **2013**, *590*, 201−207.

(53) Tan, G.; Wang, Q.; Zheng, H.; Zhao, W.; Zhang, S.; Liu, Z. Concept of variable activation energy and its validity in nonisothermal kinetics. *J. Phys. Chem. A* **2011**, *115*, 5517−5524.

(54) Smith, I. W. M. The temperature-dependence of elementary reaction rates: Beyond Arrhenius. *Chem. Soc. Rev.* **2008**, *37*, 812−826.

(55) Georgievskii, Y.; Klippenstein, S. J. Strange kinetics of the C_2H_6 + CN reaction explained. *J. Phys. Chem. A* **2007**, *111*, 3802−3811.

(56) Vyazovkin, S. Kinetic concepts of thermally stimulated reactions in solids: A view from a historical perspective. *Int. Rev. Phys. Chem.* **2000**, *19*, 45−60.

(57) Wold, S. Temperature dependence of the heat capacity of activation $(\Delta C_p^{\ddagger})$ for solvolysis reactions in water. *J. Phys. Chem.* **1972**, *76*, 369−374.

(58) Kohnstam, G. Heat capacities of activation and their uses in mechanistic studies. In *Advances in Physical Organic Chemistry*, Gold, V., Ed.; Academic Press, 1967; Vol. 5, pp 121−172.

(59) Hyne, J. B.; Robertson, R. E. On the temperature dependence of the reaction velocity. *Can. J. Chem.* **1955**, *33*, 1544−1551.

(60) The MathWorks Inc.. *MATLAB 2019*, version 2019a: Natick, MA, 2019, https://uk.mathworks.com.

(61) La Mer, V. K. Chemical kinetics. The temperature dependence of the energy of activation. The entropy and free energy of activation. *J. Chem. Phys.* **1933**, *1*, 289−296.

(62) Shannon, R. J.; Blitz, M. A.; Goddard, A.; Heard, D. E. Accelerated chemistry in the reaction between the hydroxyl radical and methanol at interstellar temperatures facilitated by tunnelling. *Nat. Chem.* **2013**, *5*, 745.